ECOSYSTEM CARBON FLUX IN A DISTURBED, FRAGMENTED SOUTHERN CALIFORNIA LANDSCAPE

John Gamon,[1,2] D. Fuentes,[3] D. Sims,[1,2] S. Houston,[2] A. Moyes,[1,2] H.-L. Qiu,[1,3] W. Oechel[4]

1. BACKGROUND

Humans are altering biogeochemical cycles in many ways. Our activities, through land use change and altered fire frequency, have measurable impacts on biogeochemical cycles, including the photosynthetic and respiratory components of the carbon cycle. Recent policy discussions concerning carbon management (e.g. Kyoto protocol) require that we develop a quantitative understanding of terrestrial carbon fluxes (i.e. the photosynthetic and respiration rates of natural landscapes).

In southern California, activities resulting from human population pressures, including land use change (e.g. urban and suburban development) and altered fire regimes (e.g. arson and fire suppression) are likely to have significant impacts on resource use and carbon flux (photosynthetic and respiratory activity) of terrestrial ecosystems. Assessing human impacts on terrestrial carbon flux is particularly problematic in this region due to fragmented land use patterns, and complex terrain. The typical measurements for directly assessing landscape-scale carbon flux (e.g. eddy covariance) require large, relatively flat and unobstructed regions to work well (Moncreiff et al., 1996). Such methods are difficult or impossible to apply in the fragmented and topographically complex terrain that characterizes much of southern California today.

An alternate method of assessing photosynthetic and respiratory carbon flux is through models derived from remote sensing. For example, a light-use efficiency model is commonly used for assessing photosynthetic carbon uptake by vegetation. Originally presented by Monteith (1977), the typical light use efficiency model expresses net primary production (NPP), or the annual accumulation of carbon via photosynthesis, as the product of two terms, absorbed photosynthetically active radiation (APAR) and the efficiency (ε) with which absorbed radiation is converted to fixed carbon:

$$NPP = \varepsilon \times APAR \qquad \text{(eq. 1)}$$

In this case, efficiency is sometimes treated as a constant for a given biome and is derived from literature values (e.g. Ruimy, 1996). However, many recent studies have demonstrated that light-use efficiency can be quite variable, particularly over the short term (days to months) and for vegetation types exposed to temperature extremes or drought stress, (Running and Nemani, 1988; Gamon et al., 1995). This view of a dynamic light-use efficiency has prompted the exploration of alternate expressions of the light-use efficiency model that are capable of defining photosynthetic activity over a finer range of temporal and spatial scales.

Alternate versions of the light-use efficiency model express instantaneous photosynthetic rate (PS) as a product of absorbed photosynthetically active radiation (APAR) and radiation-use efficiency (ε):

$$PS = \varepsilon \times APAR \qquad \text{(eq. 2)}$$

[1] Center for Environmental Analysis (CEA-CREST), California State University, Los Angeles, California 90032 (jgamon@calstatela.edu)
[2] Department of Biological Sciences, California State University, Los Angeles, California 90032
[3] Department of Geography and Urban Analysis, California State University, Los Angeles, California 90032
[4] Global Change Research Group, San Diego State University, San Diego, California 92182

APAR can be further defined as the product of incident light intensity (PAR) and the fraction of incident light that is absorbed by vegetation that is potentially available for photosynthesis (f_{APAR}).

$$APAR = PAR \times f_{APAR} \qquad \text{(eq. 3)}$$

Typically, f_{APAR} is derived from remote sensing using a vegetation index such as the normalized difference vegetation index (NDVI), which is readily available from a wide range of satellite and aircraft instruments (Gamon et al., 1995; Gamon and Qiu, 1999). Incident light intensity (PAR) can be easily obtained from meteorological stations or remote sensing. Thus, evaluation of the APAR term for large landscapes is fairly straightforward. However, evaluation of the efficiency (ε) term in equation 2 is more problematic, and is usually not possible with remote sensing. However, with hyperspectral data, it is often possible to derive ε from narrow-band indices. For example, numerous studies have shown that the photochemical reflectance index (PRI), derived from reflectance at 531 nm and 570 nm can serve as an index of light-use efficiency at leaf and canopy scales (Gamon et al, 1992; Penuelas et al., 1995; Gamon et al., 2001; Stylinski et al., 2002). Recent applications of this index using aircraft remote sensing in the boreal forest have shown some promise for deriving light-use efficiency and photosynthetic rates for whole vegetation stands (Nichol et al., 2000; Rahman et al., 2001). If this approach can be extended to a larger variety of landscapes and vegetation types, including disturbed landscapes, then it could provide a powerful tool for assessing spatial and temporal patterns of photosynthetic activity across different landscapes.

The purpose of this study was to assess patterns of carbon flux in a fragmented southern Californian landscape exhibiting various degrees and types of human disturbance. To do this, we applied a light-use efficiency model to AVIRIS imagery to generate a map of photosynthetic carbon uptake. The AVIRIS imagery was also used to derive a detailed cover-type map that, along with the photosynthesis map, was used to examine the relative productivity of different landscape regions. If this approach can be successfully validated in such a complex and disturbed region, then it could provide a way to improve our understanding of the impact of human land-use change on the carbon cycle.

2. METHODS

2.1 AVIRIS imagery

Low-altitude AVIRIS imagery of the Cheeseboro Canyon region (center longitude and latitude: 34° 9’56” N, 118° 43’ 12” W) obtained on Sept 9, 2000, was used for this analysis, yielding a “pixel size” (instantaneous field of view) of approximately 4.3 meters. The images (3.5 AVIRIS scenes from flight # f000909t01p01_r05) were processed to surface reflectance using the commercial software (ACORN, Analytical Imaging and Geophysics LLC, Boulder, Colorado). This region was chosen in part because it contains large holdings of public land (allowing access for field validation) but also because it forms a critical wildlife corridor between the Santa Monica Mountains and the Santa Susana Mountains. Changing human land use in this region, which includes suburban development, roadways and a large landfill, provided the opportunity to examine the impact of diverse land-use patterns and cover types on photosynthetic productivity, expressed as net carbon uptake of different landscape regions.

2.2 Light-use efficiency model

The light use efficiency model was developed using independent measurements primarily collected in a mature chaparral stand at San Diego State University’s Sky Oaks Reserve (San Diego County), where measurements of ecosystem photosynthesis, spectral reflectance, and stand structure are underway. At this site, spectral reflectance along a 100-m transect in the vicinity of the eddy covariance sampling was obtained using a field spectrometer (UniSpec DC, PP Systems, Haverhill Massachusetts). Reflectance data were used to model net photosynthesis according to equation 2.

NDVI (table 1) was used to derive f_{APAR} according to the following empirical calibration:

$$f_{APAR} = (NDVI \times 1.25) - 0.135 \qquad \text{(eq. 4)}$$

The values for f_{APAR} were then combined with midday light intensity (PAR, estimated to be 1740 umol m^{-2} s^{-1}) to derive APAR, according to equation 3.

Light use efficiency (ε) was derived from the photochemical reflectance index (PRI, table 1) by calibrating PRI measurements (sampled with spectral reflectance) against whole-ecosystem light-use efficiency (derived from eddy covariance measurements at midday), yielding the following equation:

$$\varepsilon = 0.034 + (PRI \times 0.447) \qquad \text{(eq. 5)}$$

The estimated LUE values were then combined with APAR estimates, as indicated in equation 2, to yield a modeled estimate of net CO_2 flux (i.e. net photosynthetic rate) for all AVIRIS scenes.

2.3 Deriving cover types

AVIRIS scenes were also used to derive a vegetation map for the region. First, a series of reflectance indices (table 1) were derived from the AVIRIS reflectance imagery. The precise bands employed in the index equations were obtained using the linear interpolation option included in ENVI 3.5 (Research Systems Inc., Boulder Colorado). The resulting index images were then combined and used in a maximum likelihood routine to map the distribution of land cover types. We used an existing vegetation map of this region, derived from a spring 1993 Landsat TM image and aerial orthophoto quadrangles (Franklin, 1997), provided by the National Park Service, to identify regions of uniform cover type to use as training sites in the maximum likelihood routine. The identity of these training sites were then confirmed by field visits. The resulting vegetation map was then used to analyze the relative flux rates of different cover classes, as shown in table 2.

Table 1 - Reflectance indices used in this study for vegetation mapping. Indices also used for deriving carbon flux are indicated with an asterisk (*).

Index	**Formula**	**Purpose**	**Reference**
Water Band Index	R_{900}/R_{970}	Vegetation water content	Peñuelas et al., 1993 & 1997
Chlorophyll index	$(R_{750}-R_{705})/(R_{750}+R_{705})$	Vegetation chlorophyll content	Gitelson & Merzlyak, 1994; Gamon & Surfus, 1999
Photochemical reflectance index*	$(R_{531}-R_{570})/(R_{530}+R_{570})$	Photosynthetic light use efficiency	Gamon et al., 1992; Peñuelas et al., 1995; Gamon et al., 2001; Stylinski et al., 2002
Normalized difference water index	$(R_{860}-R_{1240})/(R_{860}+R_{1240})$	Vegetation water content	Gao, 1996
Normalized difference vegetation index*	$(R_{800}-R_{680})/(R_{800}+R_{680})$	Fraction of light absorbed by green vegetation (F_{PAR}), potential photosynthesis	Bartlett et al., 1990; Gamon et al., 1995

3. RESULTS AND DISCUSSION

A comparison between the Landsat-derived map (Franklin, 1997) and the AVIRIS-derived vegetation map is provided in figure 1. Not surprisingly, the AVIRIS-derived map shows a much finer-grained classification due, in part, to the finer pixel size of the low-altitude AVIRIS imagery. Field surveys indicated that, in many locations, the AVIRIS imagery yielded a more accurate map. For example, the

Landsat-derived map indicated large areas of coastal sage scrub (dark green) that were often not present in the field. The AVIRIS imagery indicated that a large part of this region was actually a fairly continuous area of grassland (e.g. the north-south trending light green region in the central part of the AVIRIS-derived map in figure 1). Field surveys indicated that most of this region was indeed dominated by grassland rather than coastal sage scrub. Additionally, new regions of disturbance showed up in the AVIRIS scenes that were not visible in the Landsat-derived map produced a few years earlier. For example, the right side of the AVIRIS-derived map (figure 1) indicated a large region of disturbed land that subsequent field visits proved to be a new suburban construction site dominated by bare soil. Although a quantitative accuracy assessment has yet to be conducted, our qualitative assessment suggested that the AVIRIS map was probably an improvement over the original Landsat-derived map.

Combining information from the vegetation map (figure 1) with the carbon flux map (figure 2) allowed us to evaluate the relative photosynthetic activity of different land cover types (table 2). According to the model (figure 2), oak woodland along riparian corridors exhibited the highest net photosynthetic rate, with all other vegetation types (chaparral, coastal sage scrub, and annual grassland) exhibiting much lower rates (table 2). Lower rates for these vegetation types are consistent with previous studies, and are to be expected at the end of the summer dry season (Gamon et al., 1995). Suburban development, which consisted of a combination of houses, driveways, roads, and irrigated landscapes, exhibited a net photosynthetic rate that was approximately half (48.7%) that of the riparian oak woodland. By contrast, recently disturbed areas exhibited rates that were essentially zero or slightly negative (landfill, new development, and recently burned chaparral). If correct, negative rates would indicate that the land surface was actually a slight source of carbon to the atmosphere. In other words, respiratory activity (carbon loss to the atmosphere) was larger than photosynthetic activity (carbon gain from the atmosphere), leading to a negative *net* photosynthetic rate. However, it should be noted, that these modeled rates have not been validated yet. These relatively small percentage differences in modeled rates between landscape categories could be explained in a variety of ways, and could simply be due to errors inherent in the particular approach (e.g. errors in atmospheric correction or errors in the flux model itself).

Table 2 – relative photosynthetic activity, expressed as maximum midday photosynthetic rate, for selected cover types chosen from the AVIRIS-derived map in figure 1. Photosynthetic rates are derived from the flux image in figure 2, and are expressed as a percent of maximum rates exhibited by oak woodland in riparian corridors.

Landcover classification	**Relative photosynthetic rate (%)**
Riparian	100
Chaparral	16.6
Recently burned chaparral	-1.0
Coastal sage scrub	13.2
Grassland	-2.6
Suburban development	48.7
Disturbed (new development)	-4.9
Disturbed (landfill)	-0.6

This analysis allows us to draw several useful, if tentative, conclusions about the impact of human activity on photosynthetic productivity. Most notably, even in the best of circumstances (well-watered suburban landscapes), the photosynthetic activity of altered landscapes remains a fraction of that of riparian woodland, yet higher than other natural (unbuilt) landscapes. Presumably, surburban vegetation, which is typically heavily irrigated, has relatively high photosynthetic rates. On a leaf-area basis, these rates are most likely similar to those of riparian vegetation similarly exposed to abundant water. However, despite a presumably heavy input of water and fertilizer, the overall photosynthetic rates of suburban developments are only half that of riparian areas. Presumably, this effect is partly due to the large areas devoid of vegetation (e.g. paved areas, rooftops, and other constructed landscapes), in human-derived landscapes. Although not explicitly considered here, further analysis might attempt to examine the “resource-use efficiency” (e.g. water-use efficiency) of different landscape types. An analysis of resource-use efficiency

could take into account water and fertilizer usage in various human-derived landscapes and could compare these to nearby "natural" (unbuilt) landscapes. Such an analysis might be useful for developing strategies to maximize photosynthetic productivity of landscapes with a minimum of resource use.

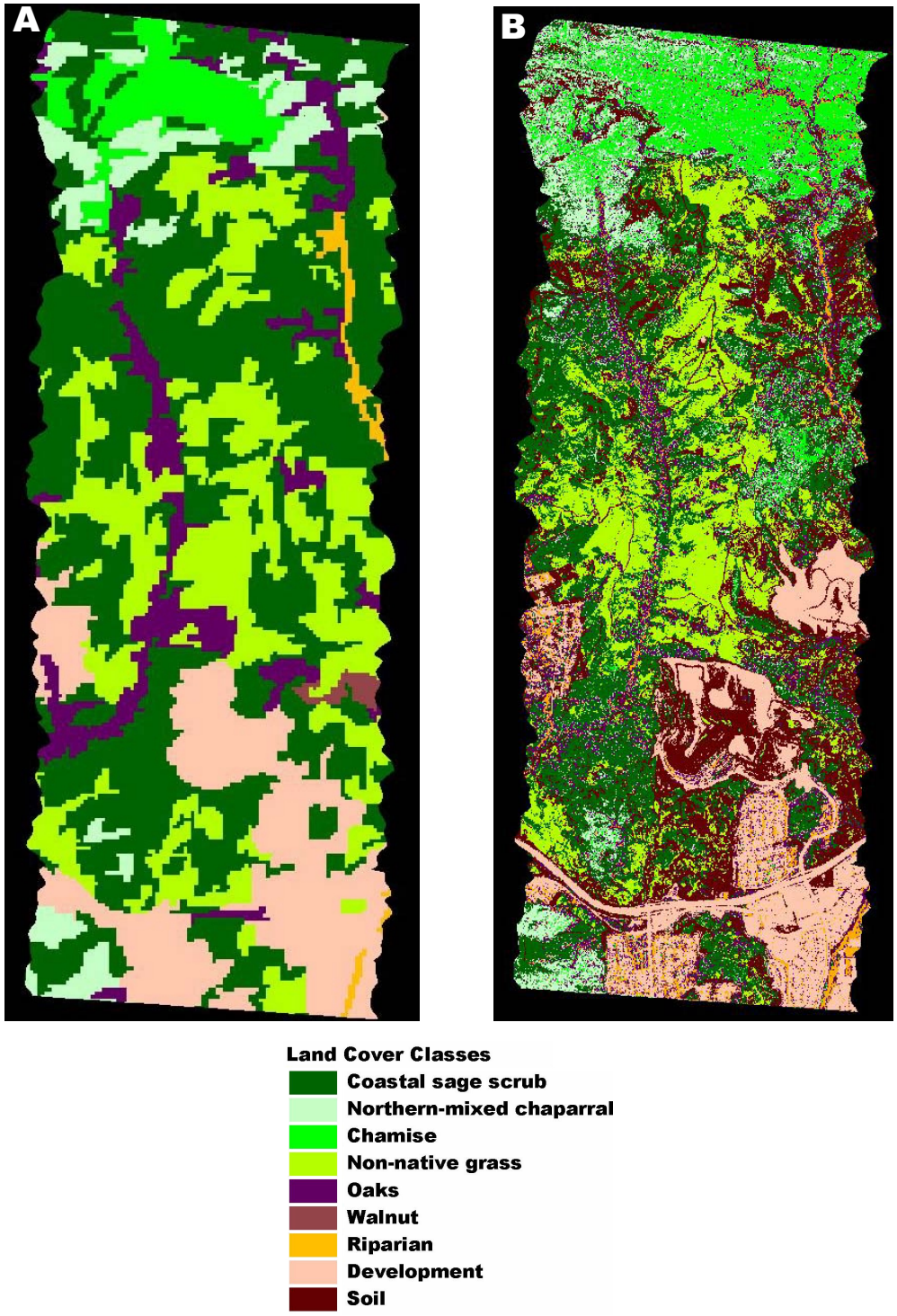

Figure 1 – Landsat-derived vegetation map (A) and AVIRIS-derived vegetation map (B) for Cheeseboro Canyon.

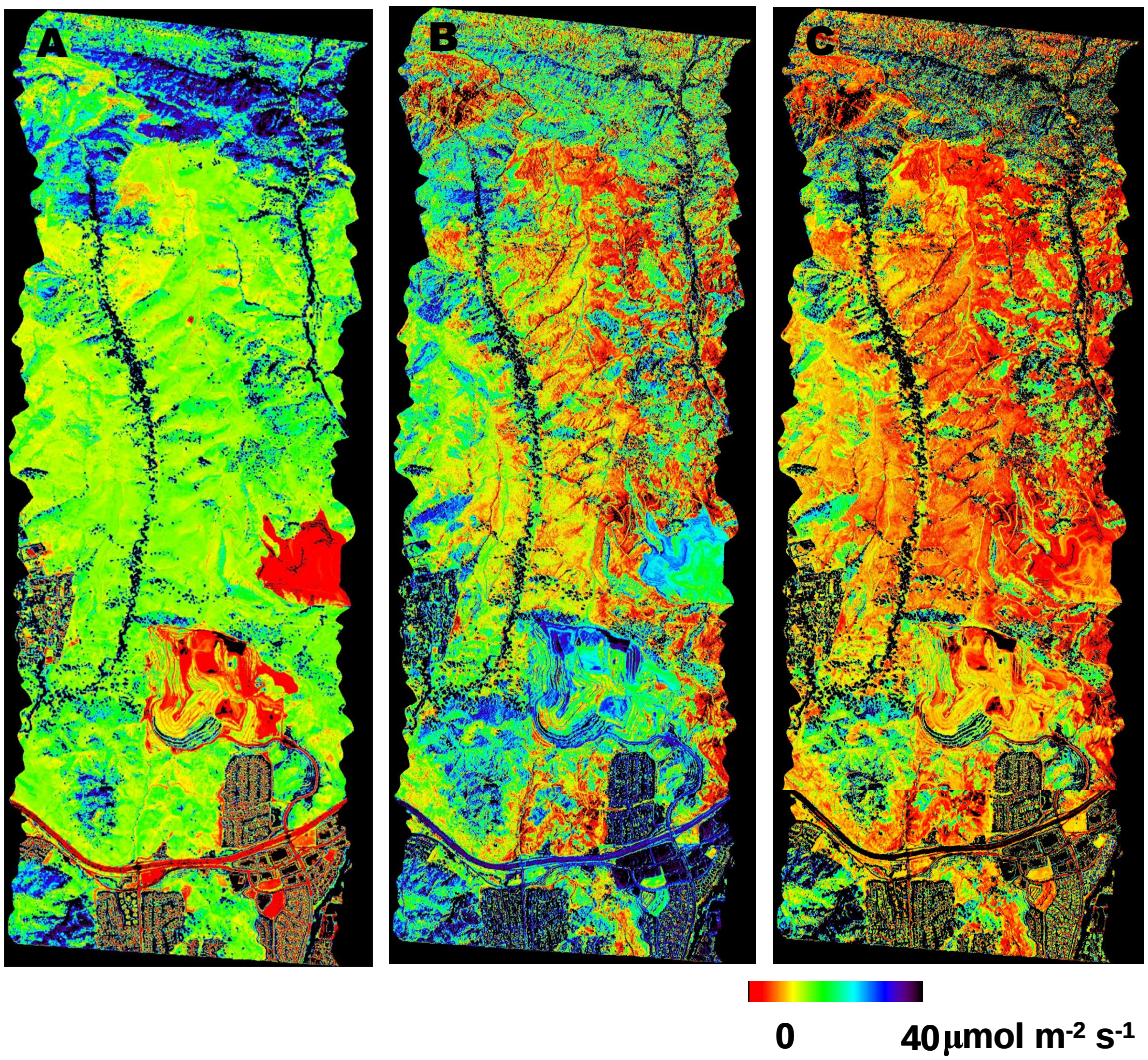

Figure 2 – Images of NDVI (A) and PRI (B) used to derive an image of midday net photosynthetic rate (C) according to the model in equation 2. In panels A and B, red indicates low values, and blue-black indicates high values (similar scale to panel C).

The analysis presented here also illustrates the value of riparian woodland. If our analysis is correct, these regions are far more productive on a land-area basis than all the built landscapes. It is well known that riparian regions also provide critical wildlife habitat, and important corridors for wildlife migration. In the case of this particular region, the riparian corridors provide a potentially critical connection between two large public land holdings, the Santa Monica Mountains, and the Santa Susana Mountains. Part of the attraction to wildlife is undoubtedly a result of its relatively high photosynthetic productivity, which provides food as well as protective cover.

It should be emphasized that the modeled photosynthetic rates reported here have not yet been validated by direct field measurements, and that a thorough validation (e.g. by direct flux measurements), would be difficult or impossible for much of this fragmented landscape, some of which is privately owned. Thus, the photosynthetic rates and conclusions presented here should be considered *hypotheses* to be tested with further study. More work is needed to develop methods of validating this approach in such a complex landscape.

4. CONCLUSIONS

The results presented here demonstrate a method for assessing cover type and photosynthetic productivity for a range of natural and human-disturbed landscapes in southern California, a region heavily impacted by human disturbance. The cover type with the highest photosynthetic productivity was riparian woodland, a cover type that also serves an important function as a wildlife corridor in this region. Suburban development exhibited the next highest photosynthetic productivity (approximately 50% of riparian woodland), but presumably at a large cost in terms of fertilizer and water usage. By contrast, recently disturbed sites (e.g. new developments, landfill, and recently burned chaparral) showed photosynthetic rates that were essentially zero or slightly negative, suggesting a possible source of carbon to the atmosphere. Future work will attempt to validate the methods and conclusions presented here, allowing us a quantitative assessment of human impacts on the carbon budget in this region.

5. ACKNOWLEDGEMENTS

We thank the staff of the Santa Monica Mountains National Recreation Area (National Park Service), for the provision of the Landsat-derived vegetation map and for logistical support in the field. We are grateful to the AVIRIS team for providing the low-altitude AVIRIS imagery. Funding for this work was provided by NSF's CREST program.

6. REFERENCES CITED

Bartlett, D.S., G.J. Whiting, J.M. Hartman, 1990, "Use of Vegetation Indices to Estimate Intercepted Solar Radiation and Net Carbon Dioxide Exchange of a Grass Canopy," Remote Sensing of Environment, vol. 10, pp. 115-128.

Franklin J. (1997) Forest Service Southern California Mapping Project. Task 11. Description and Results. Final Report. Santa Monica Mountains National Recreation Area, National Park Service.

Gamon J.A. and H-L.Qiu, 1999, "Ecological Applications of Remote Sensing at Multiple Scales, in: Handbook of Functional Plant Ecology, F.I. Pugnaire and F. Valladares editors, Marcel Dekker, Inc. New York, pp. 805-846.

Gamon J.A. and J.S. Surfus, 1999, "Assessing Leaf Pigment Content and Activity with a Reflectometer," New Phytologist, vol. 143, pp. 105-117.

Gamon J.A., C.B. Field, A.L. Fredeen, and S. Thayer, 2001, "Assessing photosynthetic downregulation in sunflower stands with an optically-based model," Photosynthesis Research, vol. 67, pp. 113-125.

Gamon J.A., C.B. Field, M. Goulden, K. Griffin, A. Hartley, G. Joel, J. Peñuelas, and R. Valentini, 1995, "Relationships between NDVI, canopy structure, and photosynthetic activity in three Californian vegetation types," Ecological Applications, vol. 5, no. 1, pp. 28-41.

Gamon J.A., J. Peñuelas, and C.B. Field, 1992, "A Narrow-Waveband Spectral Index that Tracks Diurnal Changes in Photosynthetic Efficiency," Remote Sens. of Environ., vol. 41, pp. 35-44.

Gao B.-C., 1996, "NDWI- A Normalized Difference Water Index for Remote Sensing of Vegetation Liquid Water from Space," Remote Sensing of Environment, vol. 58, pp. 257-266.

Gitelson A., and M.N. Merzlyak, 1994, "Spectral Reflectance Changes Associated with Autumn Senescence of *Aesculus hippocastanum* L. and *Acer platanoides* L. Leaves. Spectral Features and Relation to Chlorophyll Estimation," Journal of Plant Physiology, vol. 143, pp. 286-292.

Moncrieff JB, Y. Malhi Y, and R. Leuning, 1996, "The Propagation of Errors in Long-Term Measurements of Land-Atmosphere Fluxes of Carbon and Water," Global Change Biology, vol. 2, pp. 231-240.

Monteith, J.L., 1977, Climate and the Efficiency of Crop Production in Britain, Philosophical Transactions of the Royal Society of London, vol. 281, pp. 277-294.

Nichol C. J., K.F. Huemmrich, T.A. Black, P.G. Jarvis, C.L. Walthall, J. Grace, and F.G. Hall, 2000, "Remote Sensing of Photosynthetic Light Use Efficiency of Boreal Forest. Agric. Forest Meteorol., vol.101, pp. 131-142.

Peñuelas J, I. Filella and J.A. Gamon, 1995, "Assessment of Photosynthetic Radiation-use Efficiency with Spectral Reflectance," New Phytologist, vol. 131, pp. 291-296.

Peñuelas J, I. Filella, C. Biel, L. Serrano, and R. Savé, 1993, "The Reflectance at the 950-970 nm Region as an Indicator of Plant Water Status," International Journal of Remote Sensing, vol.14, pp. 1887-1905.

Peñuelas J, J. Piñol, R. Ogaya, and I. Filella, 1997, "Estimation of Plant Water Concentration by the Reflectance Water Index WI (R900/R970)," International Journal of Remote Sensing, vol. 18, pp. 2869-2875.

Rahman A.F., J.A. Gamon, D.A. Fuentes, D. Roberts and D. Prentiss, 2001, "Modeling Spatially Distributed Ecosystem Flux of Boreal Forests using Hyperspectral Indices from AVIRIS Imagery," J. Geophys. Res., vol. 106 (D24), pp. 33579-33591.

Ruimy A., G. Dedieu, B. Saugier, 1996, "TURC: a Diagnostic Model of Continental Gross Primary Productivity and Net Primary Productivity," Global Biogeochemical Cycles, vol. 10, pp. 269-285.

Running S.W. and R.R. Nemani, 1988, Relating Seasonal Patterns of the AVHRR Vegetation Index to Simulated Photosynthesis and Transpiration of Forests in Different Climates. Remote Sensing of Environment, vol. 24, pp. 347-367.

Stylinski, C.D., J.A. Gamon, and W.C. Oechel, 2002, "Seasonal Patterns of Reflectance Indices, Carotenoid Pigments and Photosynthesis of Evergreen Chaparral Species," Oecologia, vol. 131, pp. 366-374.